anisotropy in the lower frequency range is due to the difference in the mobility of the free ions and the consequent space charge polarization in the two directions. Single chain silicate minerals also exhibit similar behaviour [1].

Frequency variations of the a.c. conductivities are also similar, with minor difference in the intermediate range (Fig. 4). These may be due to the presence of traces of moisture.

Fig. 5 shows that the d.c. conductivities at different temperatures along the longitudinal direction are much higher than the conductivities in the transverse direction at the corresponding temperatures. The relatively high conductivity in the longitudinal direction and low in the transverse direction is due mainly to the regularity of structure along the axial direction and disorder in the plane perpendicular to the axis of the fibre. The high conductivity in the axial direction may probably be explained in the same way as in ionic superconductors by attributing the increased conductivity to high mobility of ions in the interchain position, similar to the Na^+ in the interlayer position in β-alumina [6]. Another interesting point to note is that the d.c. conductivities around 35° C in both the directions are of the same order as the corresponding a.c. conductivities at lower frequencies, which leads us to believe that the carriers in both cases are the same.

Acknowledgement

The authors express their sincere thanks to Professor K. V. Rao and Dr R. Bhuniya for providing the experimental facilities and many helpful discussions. Thanks are also due to Mr A. Subramaniyan for his co-operation in taking the dielectric measurements. The authors also like to record their grateful thanks to Professor G. B. Mitra of the Department of Physics for his encouragement and interest in the work.

References

1. ALDURA A. J. PIWINSKII, H. C. HEARD and R. N. SCHOCK, "The Physics and Chemistry of Minerals and Rocks", edited by R. G. J. Strens (John Wiley and Sons., London, New York, Sydney, Toronto, 1976).
2. G. R. OLHOEFT, *ibid.*
3. G. V. KELLER, "Hand book of Physics Constants", edited by S. P. Clarks, Jr. (Geological Society of America Inc., New York).
4. G. VIJAYASREE, P. S. MUKHERJEE and S. BHATTACHERJEE, *Indian J. Phys.* 50 (1976) 1052.
5. P. S. MUKHERJEE, S. BHATTACHERJEE, *Indian Miner.* 17 (1976) 49.
6. G. D. NIGAM, *Indian J. Pure Appl. Phys.* 24 1976) 215.
7. R. C. BHUNIYA, *ibid.* 9 (1971) 83.
8. A. GUINIER, *J. Phys. Ed.* 5 (1977) 1.

Received 16 September
and accepted 16 December 1977.

P. S. MUKHERJEE
A. K. DE
S. BHATTACHERJEE
School of Research in X-rays and Structure of Matter, Department of Physics, Indian Institute of Technology, Kharagpur, India 721302

Oriented growth of CoO on Co_3O_4

As part of the study of the elementary mechanisms of the thermal decomposition: $Co_3O_4 \rightarrow 3\ CoO + 1/2\ O_2$ (the interest of which relates to the wide industrial use of Co_3O_4-based catalysts) the orientation relationships between the crystal lattices of both solid phases were investigated.

So far, Colaïtis *et al.* have investigated the low temperature oxidation of finely divided CoO and reported orientation relationships depending on particle size [1].

Octahedral monocrystals (edge 2 mm) were grown by chemical transport in HCl [2]. A silica tube (200 mm long, 8 mm in diameter) containing 10 mg of Co_3O_4 (Johnson Matthey 99.998%) and a few drops of fuming HCl, was cooled in liquid nitrogen, pumped out, sealed and placed in a temperature gradient (850 to 900° C) for a week. Note that using iodine as the transport agent gave much less satisfactory results (small and poorly formed crystals) while the flux method with KCl or Na_2WO_4 yielded aggregates of tiny octahedral crystals.

The decomposition conditions were determined by the thermodynamics and kinetics of the reaction and by the requirement of a low decomposition temperature in order to reduce the oxygen

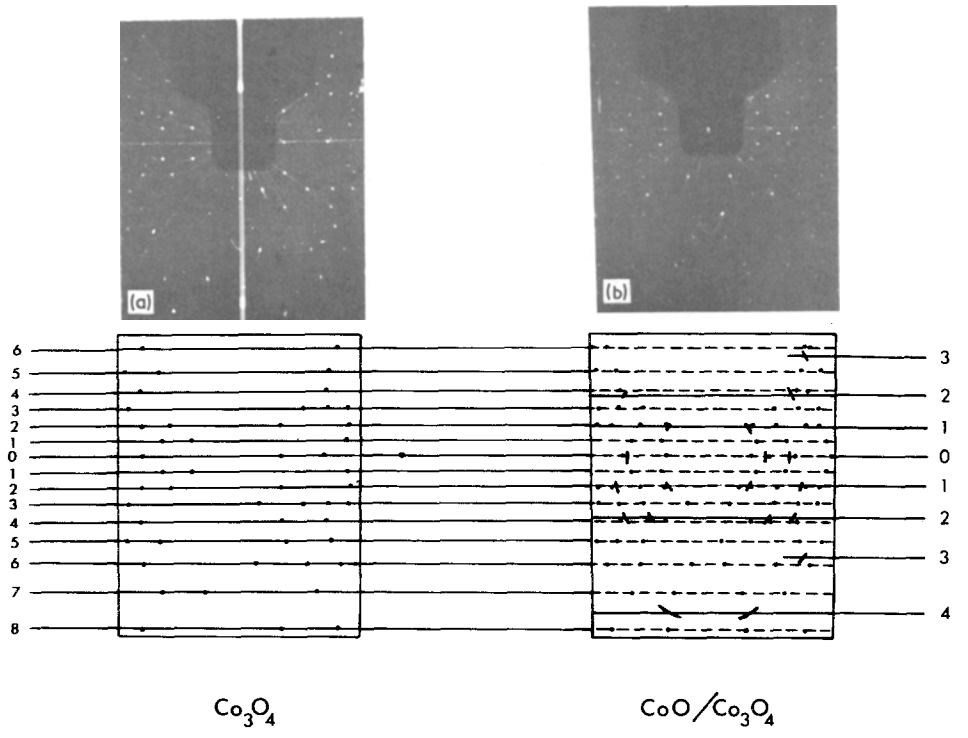

Figure 1 X-ray diffraction patterns by the oscillating-crystal method; (a) unreacted Co_3O_4 crystal, (b) partially decomposed crystal. Rotation is around [0 0 1] of the habit.

evolvement rate as well as the hindering effects of sintering of the forming CoO particles. Crystals were placed in a quartz tube connected to an ultra-vacuum system. After evacuation down to about 1.10^{-9} Torr at room temperature, the latter was raised gradually, using an external furnace, up to 645 to 650° C and maintained at that level over two days under constant pumping. In those conditions the pressure of oxygen evolved from the crystals never exceeded 2×10^{-7} Torr (the equilibrium pressure at 650° C is about 1×10^{-2} Torr). Note that, at constant temperature, the oxygen pressure in the vessel remained constant, corresponding to the balance of the evolved and pumped flows of oxygen, and although actual reaction rates could not be calculated, it might be inferred that the decomposition proceeded extremely slowly and reached a very small extent.

The orientation relationships between the structures of the parent and product phases were inferred by comparing the X-ray diffraction patterns by the oscillating crystal and the Weissenberg methods of the same crystal before and after partial decomposition. MoKα radiation and a 180 mm camera were used.

Let us remember first that Co_3O_4 crystallizes with the normal 2–3 spinel structure (SG O_h^7-FD3M) and CoO with the rocksalt structure (SG O_h^5-FM3M).

Fig. 1 shows the patterns obtained by oscillating the crystal over about ±20° around the [0 0 1] axis of its habit. For unreacted Co_3O_4, the point pattern consists of layer lines; the lattice parameter calculated from their distance is 0.8088 ± 0.0011 nm, the value expected from powder data [3]. With the reacted crystal, large additional spots due to the new phase are noted: they are actually centred on the layer lines expected assuming that the CoO structure (lattice parameter: 0.425 nm) is oriented with one [0 0 1] axis parallel with the crystal rotation axis. In addition, it was verified that the patterns obtained with the crystal set up as above but kept immobile in two positions, deduced one from the other by a rotation of 90° C, were identical. This demonstrates that both CoO and Co_3O_4 structures have a parallel four-fold

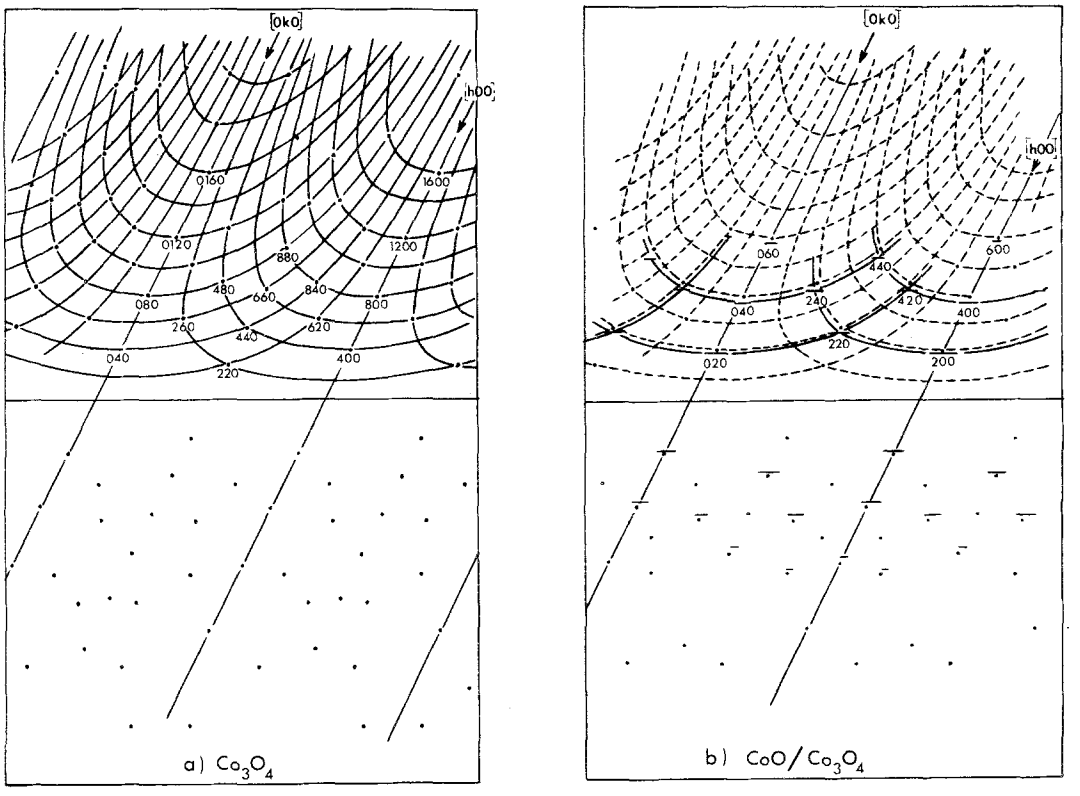

Figure 2 X-ray diffraction patterns by the Weissenberg method with layer-line "0" (of Fig. 2), (a) unreacted Co_3O_4 crystal, (b) partially decomposed crystal. Rotation is around [0 0 1] of the habit. In the upper part of Pattern b, the dashed curves connect together the Co_3O_4 reflections and the full curves the indexed reflections due to CoO.

symmetry axis:

$$[0\,0\,1]_{CoO} \parallel [0\,0\,1]_{Co_3O_4}.$$

The orientations in the (0 0 1) plane were established using the Weissenberg method. Fig. 2 shows reproductions of the point patterns thus obtained with the crystal set up as above and developing the zero layer-line of the patterns in Fig. 1. The structures and lattice parameters of both solid phases being known, indexing the observed reflections was quite easy: thus, the lattice parameter of Co_3O_4 being about twice that of CoO, and most extinction conditions being the same in both space groups, any (low index) CoO reflection almost coincides with the Co_3O_4 reflection with double indexes (for example 220 CoO and 440 Co_3O_4). The obvious result of the experiment is thus to show that the other two four-fold symmetry axes in one structure are parallel to the equivalent axis in the other:

$$[1\,0\,0]_{CoO} \parallel [1\,0\,0]_{Co_3O_4}$$

$$[0\,1\,0]_{CoO} \parallel [0\,1\,0]_{Co_3O_4}.$$

The most simple orientation relations thus established mean that any direction or plane in one structure is parallel to its equivalent in the other structure, which can be best summed up as follows:

$$CoO\,(0\,0\,1)_{\langle 1\,0\,0\rangle} \parallel Co_3O_4\,(0\,0\,1)_{\langle 1\,0\,0\rangle}.$$

Now, in both structures, anions form a face-centered-cubic sublattice (the O–O distance being 0.202 nm in Co_3O_4 and 0.212 nm in CoO). Consequently, the mechanism of the reaction (i.e. the atomic movements taking place in the solid state and leading to the formation of the nuclei of the new phase) can be best described in terms of cation reordering in an interfacial layer in which the oxygen sublattice is common to both structures. That mechanism shall be detailed in our

next publication. On the other hand, the important parameter mismatch between the oxygen sublattices of both structures (about 5% linear) induces important mechanical strains, the relaxation of which was observed to occur (for reaction extents higher than in the present case) as spontaneous cleavages predominantly on (0 0 1) type planes of the crystals habit, that is on (0 0 1) type planes of both structures.

References

1. D. COLAÏTIS, F. FIEVET-VINCENT, J. GUENOT and M. FIGLARZ, *Mater. Res. Bull.* 6 (1971) 1211.
2. K. NAGASAWA, Y. BANDO and T. TAKADA, *Bull. Chem. Soc. Japan* 44 (1971) 1577.
3. H. E. SWANSON, M. I. COOK, T. ISAACS and E. H. EVANS, *Nat. Bur. Stand., Circular 539 (9)* (1960) 28.

Received 14 November
and accepted 19 December 1977

L. BERTHOD
P. BRACCONI
L. C. DUFOUR
N. FLOQUET
Laboratoire de Recherches sur la Réactivité des Solides, Faculté des Sciences Mirande, BP 138 21004, Dijon CEDEX, France

Observation of transgranular slip in an austenitic stainless steel

In recent years, a considerable amount of effort has been directed at producing theoretical models for transgranular slip; i.e. the passage of crystal deformation from grain to grain across the boundary which separates them [1–6]. In this short note, we present some examples of transgranular slip observed in thin foils of a 20% Cr–25% Ni austenitic stainless steel. During the course of the present investigation transgranular slip has only been observed when the two active slip planes (one in either grain) and the grain boundary have a common zone axis. This condition allows the passage of crystal slip from one grain to the other without any rotation of the dislocation line vector as it crosses from Grain A to Grain B. Similarly, unambiguous evidence of transgranular slip was restricted to the case where dislocation motion occurred during or after foil preparation and not in the bulk specimen. In the former case, stress relations at the foil surfaces allow dislocations to move more easily, whilst the position and orientation of the slip bands formed are defined by the slip traces at the foil surfaces.

Fig. 1 shows an example of transgranular slip (from Grain A to Grain B). In this instance an array of grain-boundary dislocations is observed on one side of the slip plane–boundary intersection. This array of dislocations arises by the following dislocation reaction:

$$\mathbf{b}_A \longrightarrow \mathbf{b}_B + \mathbf{b}_{gb}$$

where $\mathbf{b}_A$ and $\mathbf{b}_B$ are the matrix Burgers vectors in Grains A and B, and $\mathbf{b}_{gb}$ is the Burgers vector of a residual boundary dislocation. A further example of this type of reaction is given in Fig. 6 of Howell *et al.* [7]. It should be noted that the residual boundary dislocations will not, in general, be glissile. Progressive transgranular slip generated by a single active slip plane on one side of the boundary will only occur when diffusive fluxes allow associated climb and glide of the residual boundary dislocations away from the slip plane–boundary intersection. A further example of transgranular slip is shown in Figs. 2a to 2c. For this case, however, the passage of crystal slip from Grain A to Grain B has resulted in the emission of dissociated dislocations rather than total dislocations. This observation was common to many of

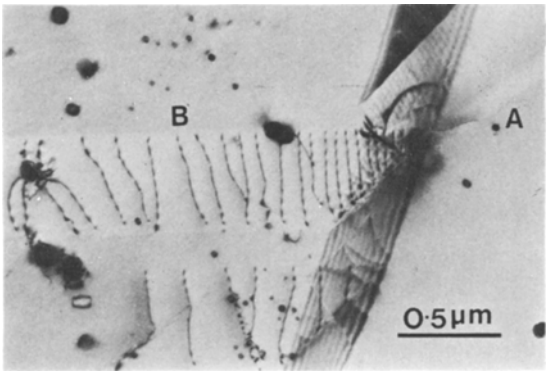

Figure 1 Transgranular slip across a high-angle grain boundary. An array of grain-boundary dislocations is observed on one side of the slip plane–boundary intersection.